Adaptive Pneumatic Force Actuation and Position Control[1]

J. E. Bobrow

F. Jabbari

Department of Mechanical Engineering,
University of California, Irvine,
Irvine, Calif. 92717

In this paper an implementation of an adaptive control law for a pneumatic actuator is presented. Pneumatic actuators are of particular interest for robotic applications because of their large force output per unit weight, and their low cost. Stabilization of a pneumatic actuator is difficult if a high bandwidth closed-loop system is desired. This is because of the compressibility of air, and of the nonlinear characteristics of air flowing through a variable area orifice. Further complications arise from the geometry of the mechanism because the equations of motion are highly nonlinear. The order of the dominant dynamics is shown to vary with the position of the mechanism.

1 Introduction

During the past decade, system identification techniques and adaptive control theory have matured to the stage that a comprehensive treatment of the approach can be found in several textbooks (Goodwin, 1984; Landau, 1979; Ljung; and Soderstrom, 1983). However, relatively few successful experimental applications have been reported in the literature. Some experiments have been conducted with good results for first or second order systems, while other higher order systems have required further refinements to be made (Rovner, 1987). In this paper, an implementation of an adaptive control law for a pneumatic actuator is presented. An approximate model for simulation purposes is derived, and both numerical and experimental results are presented.

Pneumatic actuators are of particular interest for robotic applications because of their large force output per unit weight, and their low cost. Unfortunately, stabilization of a pneumatic actuator is difficult if a high bandwidth closed-loop system is desired. This is due both to the compressibility of air, and to the highly nonlinear flow characteristics of air through a variable area orifice. A further complication arises from the geometry of the mechanism because the equations of motion are highly nonlinear. In addition, complications in modeling arise from the dynamic characteristics of the servovalve which meters the air flow, and from the assumption that the air pressure changes uniformly in the chambers. The actual air pressure response occurs during the time it takes an acoustic wave to travel the length of the actuator (Mannetje, 1981), so unmodeled dynamics are present in the system.

Because of the form of the uncertainties in the nonlinear model of the system, it is difficult to factor out all of the unknown parameters from the equations of motion, and treat these as unknown quantities to be identified. This approach is commonly used in robotics research to identify unknown mass properties of a manipulator (Slotine and Li, 1987; Craig et al., 1986; Sadegh and Horowitz, 1987). In these approaches, a set of unknown parameters are estimated using either a least squares approach, or Liapunov stability to update their values.

We used a linear ARMA (autoregressive moving average) model for the system, and identified the coefficients using a standard least squares approach (Goodwin, 1984). The control compensator was designed from the estimated model using pole-placement. Problems in the system identification were encountered due to unmodeled dynamics and to the finite resolution of our position sensor. The problem of unmodeled dynamics was carefully examined using a variable-order lattice filter (Jabbari and Gibson, 1988). The order of the dominant dynamics was shown to vary with the position of the mechanism. The problem of sensor resolution or noise was the most difficult to handle because the resulting model identified online was incorrect. We found that if we underestimated the order of the system more satisfactory performance and stability was achieved.

2 System Dynamics

2.1 Rigid Body Dynamics. A schematic representation of the one-degree-of freedom arm used for the experiments is shown in Fig. 1. It is assumed that the arm has inertia J about fixed point O, and total mass m, with the center of gravity located a distance l_1 from the pivot as shown. The force F which supports the arm is produced by the pneumatic actuator, and is collinear with the line connecting points A and B. The constants l_2, l_3, l_4, l_5 are fixed length offsets due to the geometry of the hardware, and the dimension $y+c$ is the cylinder position plus a constant.

Summing the moments about fixed point O yields the equation of motion

$$J\ddot{\beta} + g(\beta) = Fr(\beta) \tag{1}$$

where J is the moment of inertia of the arm about fixed point

[1]This research was supported by Parker-Hannifin, Parker-Bertea Aerospace Division.

Contributed by the Dynamics Systems and Control Division for publication in the JOURNAL OF DYNAMIC SYSTEMS, MEASUREMENT, AND CONTROL. Manuscript received by the Dynamic Systems and Control Division September 23, 1988. Associate Editor: D. Hullender.

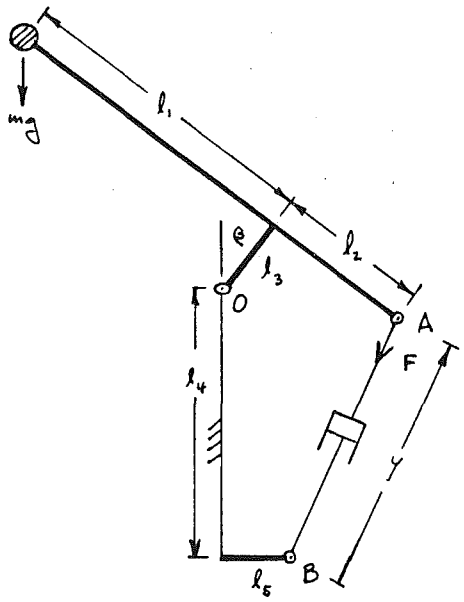

Fig. 1 The mechanism used for the experiments

O, $g(\beta) = mg(l_1 \cos \beta - l_3 \sin \beta)$ is the torque due to gravity, and the moment arm

$$r(\beta) = [\sin \beta(l_3 l_4 - l_2 l_5) + \cos \beta (l_3 l_5 + l_2 l_4)]/y,$$

with

$$y = \sqrt{l_2^2 + l_3^2 + l_4^2 + l_5^2 + 2 \cos \beta(l_3 l_4 - l_2 l_5) - 2 \sin \beta (l_3 l_5 + l_2 l_4)}.$$

Note that if $\beta = 0$, and $l_2 = l_5$, then $g(0) = mgl_1$, and $r(0) = l_2$.

2.2 Pneumatic Flow Equations. A schematic representation of the pneumatic actuator and servovalve is shown in Fig. 2. The relationship between mass flow rate of air and the change of pressure in chamber A (or chamber B) can be found using conservation of energy (Shearer, 1956; Liu and Bobrow, 1988) as

$$\dot{m}_a T_s - \frac{p_a \dot{v}_a}{c_p} + \frac{\dot{Q}}{c_p} = \frac{c_v (p_a \dot{v}_a)}{c_p R}, \tag{2}$$

where $\dot{Q}$ is the rate of heat transfer to the cylinder, $\dot{m}_a$ is the mass flow rate of air, c_v and c_p are the constant volume and constant pressure specific heats of air, R is the universal gas constant, v_a is the volume of chamber A, y is the position of the piston (Fig. 2), T_s is the air supply temperature, and p_a is the cylinder pressure. A similar equation holds for chamber B.

For this research, it is helpful to approximate the two flow equations as one first-order equation plus a small disturbance term. The first order equation relates the pressure difference, or force, on the piston to the voltage input to the servovalve. This approximation is justified here analytically and has also been verified experimentally. When the motion of the piston is slow ($\dot{y} \approx 0$) relative to the change in air pressure, and no heat is transferred to the system, the flow equation for chamber A is

$$\dot{m}_a = \frac{c_v A y}{c_p R T_s} \dot{p}_a, \tag{3}$$

where A is the piston area, so the volume of chamber A is $v_a = Ay$. The pressures in chambers A and B are assumed to change uniformly throughout the volumes. Similarly, the air flow dynamics of chamber B is

$$\dot{m}_b = \frac{c_v A (st - y)}{c_p R T_s} \dot{p}_b, \tag{4}$$

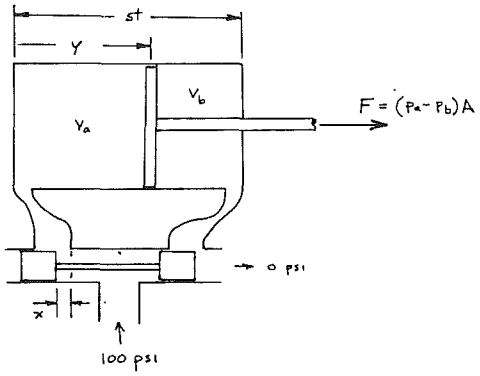

Fig. 2 The actuator and servovalve geometry

where st is the cylinder stoke (Fig. 2). We have assumed the areas on both sides of the piston are equal even though the rod on one side reduces the area on that side by a small amount. This was done to keep the equations more manageable, and does not alter the results of the identification algorithm used since the true system dynamics are found.

The flow in and out of the four-way servovalve is determined by the orifice opening x, and can be linearized (Liu and Bobrow 1988) as

$$\dot{m}_a = c_1 x + d_1 \tag{5}$$

$$\dot{m}_b = -c_1 x + d_2 \tag{6}$$

where the constants c_1, d_1, and d_2 depend on the valve opening x, the air supply pressure, and the servovalue geometry. The constants d_1 and d_2 become zero for supersonic flow through the orifice, or when the nominal operating joint for x is zero, as is the case for this research. The supersonic flow condition occurs when the ratio of the downstream pressure to the upstream pressure is less than .528, that is, $p_a/p_s < .528$ or $p_b/p_s < .528$, where p_s is the valve supply pressure.

The valve orifice opening x is created by applying a voltage to an electromagnet which causes a flapper valve to move the spool a distance x (Ogata, 1970). The bandwidth of the servovalve used was found experimentally to be approximately 30 Hertz, so these dynamics were not included in the lower frequency dynamic model of the system. Hence, the input voltage to the valve is assumed to be directly proportional to the servovalve orifice opening x.

3 Analog Pressure (Force Control)

In many robotic applications, it is desirable to directly control the actuator force F in (1) rather than the arm position. This is the case when a specified end-point force is desired, as for many assembly operations. An analog pressure control system was designed for this purpose, and also to allow the position control system, which is digital, to run at a slower sampling rate. The control computer sends commands to the analog pressure control system, which in turn applies a voltage to the servovalve to produce the desired force. To obtain position control, the joint angle is input to the computer, and the compensated error signal is output to the force control system.

To design the force control system, combine (3)–(6) to obtain $\dot{F} = h(x)$ as follows

$$\dot{F}/A = \Delta \dot{p} = \dot{p}_a - \dot{p}_b$$

$$= \frac{\dot{m}_a}{Ky} - \frac{\dot{m}_b}{K(st - y)}$$

$$= \frac{c_1 stx}{Ky(st - y)} + d,$$

where $K = c_v A / c_p R T_s$ and $d = d_1(st - y) - d_2 y / Ky(st - y)$ is a small disturbance because the nominal values of d_1 and d_2 are zero. To cause $\Delta p = p_a - p_b$, to be a desired pressure Δp_d, a proportional controller of the form

$$x = k_p(\Delta p_d - \Delta_p) \tag{8}$$

can be used to obtain the closed-loop system (combine with (7))

$$\dot{\Delta p} = \frac{c_1 s t k_p}{Ky(st - y)} (\Delta p_d - \Delta p) + d. \tag{9}$$

Hence, if the effects of d are small relative to the gain k_p, the steady-state value is $\Delta p = \Delta p_d$ as desired. If it is assumed that the position y changes slowly, the time constant for this first order system is

$$\tau = \frac{Ky(st - y)}{c_1 s t k_p}, \tag{10}$$

and the transfer function for the analog position controller is

$$\frac{\Delta p}{\Delta p_d} = \frac{1}{\tau s + 1}. \tag{11}$$

Equation (10) shows the effect of the cylinder position y on the time constant τ of the analog pressure control system. At midstroke position $y = st/2$ and $\tau = K_{st}/2c_1 k_p$ is at its maximum value so the response time is slowest in this position. As y approaches either end of the cylinder $y = 0$ or $y = st$, the time constant approaches zero. The occurrence of this change in time constant with position was confirmed experimentally. At either end of the piston's stroke the pressure controller responds very quickly, and the system becomes unstable if k_p is too large. Although (9) does not predict instability for any value of k_p, the unmodeled dynamics and saturation nonlinearities dominate the response near the ends of the stroke if k_p is too large.

Equations (1) and (9) indicate the nonlinear behavior of both the actuator dynamics and the mechanism dynamics. The position β of the arm is related to the position y of the cylinder in (1), so the equations can be written with either of these coordinates as the independent variable. Because the nonlinearities are position dependent, an adaptive controller based on linearized dynamics should be appropriate for this application. That is, the arm position changes slowly in comparison to the other state variables so there should be time to adapt to these changes. The following section describes the computer implementation of the adaptive controller.

4 Computer Hardware and Software

The adaptive control software runs on two processors, a PC-AT and a Definicom Systems DSI-020 board which runs in parallel to the PC in one of its expansion slots. The PC is used to initiate the adaptation, and to input and output the data. All the control and adaptation computations are done on the DSI-020.

The PC-AT is an 8 Mhz Intel 80286 with a floating point coprocessor, Intel 80287. A 12 bit Metrabyte digital to analog converter with a 3 microsecond conversion time was used to output the control voltage to the analog pressure control system. A 1000 line incremental encoder with a resolution of 4000 pulses per revolution (after decoding the two quadrature outputs) was used to measure the joint angle of the arm. The quadrature outputs from the encoder are counted with a Hewlett Packard HCTL 2000 chip whose output is mapped directly to the PC's I/O bus.

The Definicom Systems DSI-020 board uses a MC68020 CPU running at 20 Mhz with a MC68881 floating point coprocessor. It has a separate memory area of four Megabytes of RAM on board. A portion of this memory was allocated for communication between the PC and DSI-020. A combination of assembly language programs and C programs were written for both processors to implement the control algorithm (Nagarajan, 1988). An interrupt driven program is loaded resident in the PC, but runs independently from other programs executed from DOS, similar to the BIOS (Norton, 1985). The resident program uses the interrupt generated by the system clock to execute the adaptive control software, and can be set to run at any sampling rate from 18.2 Hz to 2000 Hz in multiples of 18.2 Hz. When the system clock generates the interrupt, the following events occur:

(a) The current contents of the 80286 are stored–i.e., the values in the registers and pointers are saved.

(b) A C subroutine is called which inputs the current joint position, transfers this data to the DSI-020 and initiates the adaptive control update routine on that board.

(c) The PC then waits for the DSI-020 to return the new control input, which is evaluated from the discrete-time compensator equation. That is, the DSI-020 takes the current position and evaluates the control law (to be discussed in the next section)

$$L(q^{-1})u = -P(q^{-1})e \tag{12}$$

where q^{-1} is the backward shift operator, $-P(q^{-1})/L(q^{-1})$ is the compensator transfer function, and $e(k) = y(k) - y_d(k)$ is the position error at sampling time k. After evaluating the control $u(k)$, the DSI-020 transfers its value to the PC.

(d) When the PC obtains the control $u(k)$ in step (c), the value is output to the D/A converter.

(e) The registers and pointers are restored in the 80286, and control of the cpu is returned to DOS.

(f) After evaluating the control law in step (c), the DSI-020 updates the new parameter estimates and the control compensator as described in the following section. This step occurs in parallel to steps d, and e, since no interaction is needed between the two processors after step c.

The most time consuming computation occurs in step (f), where the adaptive control equations are evaluated. Steps a–e require only about 1 millisecond to complete because they are mainly input and output of data. The control computation in step c is done in double precision floating point arithmetic, but the time required for this is negligible in comparison to that required for the other steps. We used a sampling rate of 91 Hz in the experiments, so the PC spends less than one tenth of its time servicing the I/O boards, and initiating action on the DSI-020. In the remaining time, the PC is free to execute DOS level routines.

Because it is desirable to monitor and modify the behavior of the controller, we also developed an interface to the memory resident adaptive control program using a DOS software interrupt INT 60H. This allows us to change control parameters and gains as the process is occurring using a high level C program. In addition, quantities such as the input $u(k)$, output $y(k)$, and the trace of the covariance matrix can be viewed and plotted in real time. Since the DOS interrupt has a lower priority than the control interrupt, no disruption of normal operation of the control law occurs.

5 System Identification

The equations of motion (1), (9) for this system are nonlinear, but they can easily be linearized for small motions about some desired operating position. Hence, the first set of experiments were to use a fixed gain lead compensator and excite the closed-loop system with a desired reference position which was a linear combination of a slow 2 Hz sine wave and a faster 50 Hz sine wave. The amplitude of the slow sine wave was small enough to assume that the system's response was approximately linear. The input/output data were collected, and the identification was done off-line. The input to the system was actually taken as the output of the fixed gain compensator

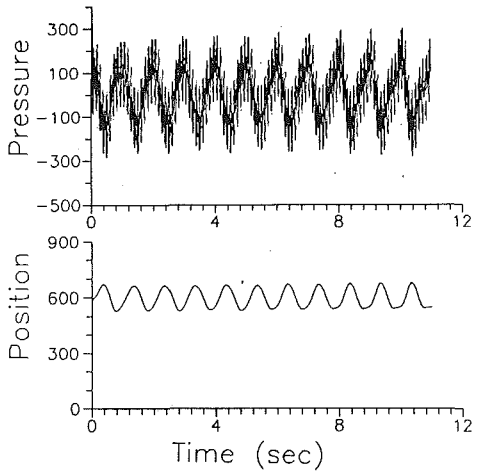

Fig. 3 Example file of input (upper) and output (lower) data

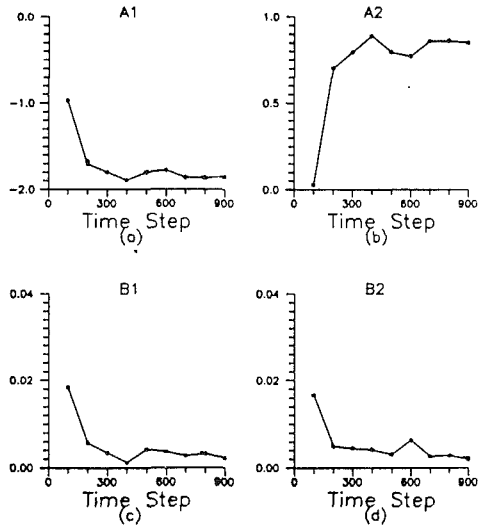

Fig. 4 System parameter estimates assuming the order is two

because it is the linearized open-loop dynamics that we would like to identify.

An example of the experimental input/output data taken is shown in Fig. 3. Note that the system behaves much like a low-pass filter. Also, the amplitude of the output sine wave is about 70 counts of the encoder which corresponds to $70\,\frac{360°}{4000}=6.3°$. Using these data, the recursive least squares algorithm with a constant forgetting factor was used to identify the dynamics. The form of the ARMA model is

$$A(q^{-1})y=B(q^{-1})u, \tag{13}$$

where $A(q^{-1}) = 1 + a_1q^{-1} + a_2q^{-2} + \ldots a_nq^{-n}$ and $B(q^{-1}) = 0 + b_1q^{-1} + b_2q^{-2} + \ldots b_nq^{-n}$. Equation (13) can also be written as

$$y(k+1)=\theta^T\phi(k), \tag{14}$$

where $\theta = [a_1, a_2, \ldots a_n, b_1, b_2, \ldots b_n]^T$, $\phi(k)=[-y(k), -y(k-1), \ldots, -y(k-n+1), \quad u(k), \quad u(k-1), \ldots, u(k-n+1)]^T$, and n is in the order of the system. The least squares cost function is

$$J_N(\hat{\theta}=\sum_{k=1}^{N}\lambda^{N-k}(y(k)-\hat{\theta}^T\phi(k-1))^2, \tag{15}$$

where $\hat{\theta}$ is the estimate of the model parameters θ, and $\lambda\leq 1.0$ is a constant forgetting factor. The cost function $J_N(\hat{\theta})$ can be minimized recursively by updating $\hat{\theta}$ (Goodwin, 1984) using

$$\hat{\theta}(k+1)=\hat{\theta}(k)+\frac{P(k-1)\phi(k)}{\lambda+\phi(k)^TP(k-1)\phi(k)}[y(k+1)-\hat{\theta}(k)^T\phi(k)], \tag{16}$$

where

$$P(k)=\left(P(k-1)-\frac{P(k-1)\phi(k)\phi(k)^TP(k-1}{\lambda+\phi(k)^TP(k-1)\phi(k)}\right)/\lambda. \tag{17}$$

We used λ's between .95 and .99 for most of our experiments, and did not observe much of a change in the performance of the system for values in this range.

To use this identification algorithm, the order of the system must be specified. As mentioned in Section 2, if the two flow equations are approximated by (9), the order of the system is 3, otherwise the order of the dominant dynamics is 4. Recall that these equations neglect higher order dynamics of the servovalve and the acoustic pressure waves in the air. When we applied the least-squares algorithm to the data shown in Fig. 3 assuming a fourth order model, we found that the parameter estimates (the $a_i's$ and $b_i's$) did not even come close to converging upon any value. Many sets of input/output data were used and similar behavior was observed. When the assumed model order was three, this was still the case. When the assumed model order was two, the parameter estimates still varied, but seemed to be converging on some values. An example plot of the estimated parameters for a second order system as they varied with each time step is shown in Fig. 4.

We found that we could easily simulate this problem using a linear analytical model. This is done by approximating the dynamics (1) with the model $F=\hat{J}\ddot{\beta}$ and fixing τ in (11). Then we set the constants $\hat{J}$ and τ to be close to the correct linearized values for this system. The discrete-time model which relates the input Δp_d (11) to the output β for this third order linear system is found by using a zero-order-hold on Δp_d. The discrete-time ARMA coefficients θ for this linear system are

$$a_1=-2-e^{-T/\tau}$$

$$a_2=1+2e^{-T/\tau}$$

$$a_3=-e^{-T/\tau}$$

$$b_1=\frac{(1-e^{-T/\tau})\tau^2}{\hat{J}}-\frac{T\tau}{\hat{J}}+\frac{T^2}{2\hat{J}}$$

$$b_2=\frac{2\tau^2(e^{-T/\tau}-1)}{\hat{J}}+\frac{T\tau(1+e^{-T/\tau})}{\hat{J}}\,\frac{T^2(1-e^{-T/\tau})}{2\hat{J}}$$

$$b_3=\frac{(1-e^{-T/\tau})\tau^2}{\hat{J}}-\frac{T\tau e^{-T/\tau}}{\hat{J}}-\frac{T^2e^{-T/\tau}}{2\hat{J}}, \tag{18}$$

where T is the sampling interval.

When a simulated input was applied to this linear model, the correct parameters in (18) were obtained using the least squares algorithm to identify them. However, to more closely approximate the behavior of our system, the finite resolution of the position encoder must be taken into account. This is done by scaling $\hat{J}$ so that the units of β are counts of the encoder (4000 pulses/revolution) and truncating the value of the analytical output to be an integer at each time step. This introduces noise to the measurement which is uniformly distributed between zero and one. With this form of sensor noise added to the simulated system, the parameter identification algorithm behaves very similar to the way it does for the actual pneumatic system.

Further insight is obtained if a lattice filter approach (Jabbari

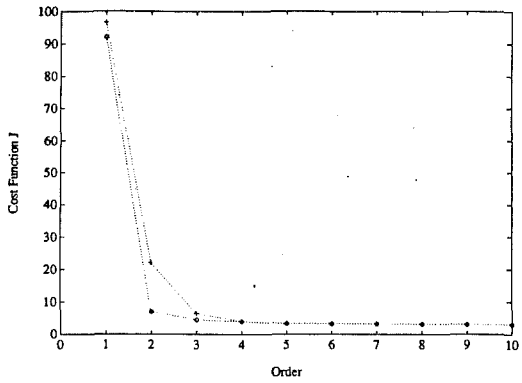

Fig. 5 The performance index versus order for two different data sets. The upper plot is data taken at the midstroke position of the cylinder.

and Gibson, 1988) is used to find the $\hat{\theta}$ vector which minimizes J_N in (15). Although the same performance index is minimized, the lattice formulation is recursive in order as well as time so models of different orders can be extracted at each time step. In addition, the value of performance index $J_N(\hat{\theta})$ can be determined easily at each time step. The upper plot of Fig. 5 shows $J_N(\hat{\theta})$ evaluated at time step 300 for different order models obtained from the actual experimental data of Fig. 3. The value of J_N gives an indication of how well the estimated model fits all of the data points taken up to time step 300 with a lower value indicating a better fit. Note that a second order model fits the data much better than a first order model, and only a small improvement occurs when a fourth order model is used rather than a third. This is in agreement with our statement that a good model is obtained for this system using (1) and (9).

The lower plot of Fig. 5 was for another set of input/output data where the nominal value of the output was chosen as 200 rather than 600 as in Fig. 3. Since the position $y=600$ corresponds to the midstroke position of the cylinder, the time constant τ from (10) is largest in this position. This explains why the lower plot of Fig. 5 shows that a better fit is obtained for a lower order model. At $y=200$, (10) shows that τ is about 55 percent of its value in the midstroke position. Hence the dynamics of the pressure control system will have a less noticeable effect in this position than in the midstroke position.

6 Adaptive Control

The ARMA coefficients identified using the least squares algorithm can be used to design the control compensator (12) using pole-placement or a model reference approach (Goodwin, 1984). For our first experiments, we tried MRAC, and were unsuccessful in obtaining a stable system unless the reference model was very slow. The problem may have been due to unstable zeros, as suggested in (Astrom, 1984). We then tried pole-placement as follows. From (12) and (13), the characteristic equation of the closed loop system is

$$LA + BP = A^*, \tag{19}$$

where $A^*(q^{-1})=0$ contains the desired closed-loop poles. The roots of A^* can be specified in several ways, and we experimented with many of them. The method which worked best was to specify reasonable values for the desired dominant roots in the continuous time s plane, and use the mapping $z=e^{sT}$ to determine their location in the z plane. The remaining roots were specified to lie on the real z axis, and their magnitudes were chosen to be smaller than the desired dominant roots.

To solve (19) for L and P, equating coefficients of q^{-1} gives a linear equation in $2n$ unknowns of the form (Goodwin, 1984)

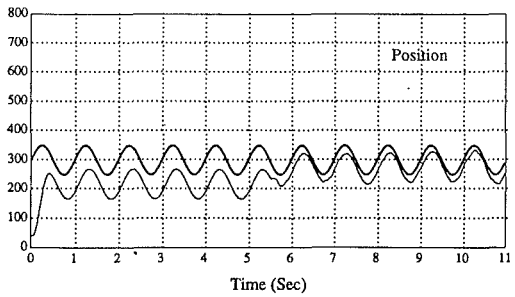

Fig. 6 The adaptive control law is activated after five seconds. The nominal angle is $\beta = 300$.

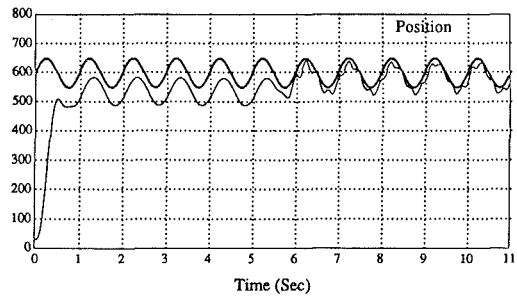

Fig. 7 Same as Fig. 6 except that nominal position is $\beta = 600$ (midstroke)

$$M\begin{Bmatrix} l \\ p \end{Bmatrix} = a^*, \tag{20}$$

where the vectors l, p and a^* are coefficients of the polynomials $L(q^{-1})$, $P(q^{-1})$, and $A^*(q^{-1})$, respectively. The vectors l and p are obtained by inverting the $2n \times 2n$ matrix M, and multiplying by a^*. Because of the fast computation speed of the DSI-020 coprocessor, we were able to update the estimate $\hat{\theta}$ using (16) and (17), and solve (20) for the new compensator L and P each time step.

Figures 6 and 7 show experimental results of the adaptive control algorithm. For these cases, a fixed gain lead compensator was used for the first 5 seconds. After this time the system parameters were updated according to (16) and (17), where it was assumed that the system order was two, and (20) was used to solve for a new compensator after each time step. The desired position is the upper bold sine wave, the output is the lower wave. The steady-state offset in the two plots is mainly due to gravity.

Note the distinct high frequency component in the response plot of Fig. 7. This suggests that a higher-order system and compensator should be used to obtain the desired closed-loop response. This is consistent with our statement that the dominant system dynamics change with position. When the order of the model was increased to three the system became, at best, marginally stable. Even though a higher order model is needed to describe the dynamics, the model obtained from the identification algorithm is not adequate for control purposes. As stated earlier, the problem is due to the finite resolution of the position sensor. We are currently investigating alternative identification algorithms to overcome the problem of sensor resolution.

7 Conclusion

A dynamic model of a pneumatic actuator has been derived, and experiments using an adaptive control algorithm have been presented. Better performance was achieved when the control law was obtained from pole-placement, rather than a model

reference approach. It was observed that the finite resolution of the position sensor used created difficulties for the system identification portion of the adaptive controller. If the assumed model order was less than the actual order, the resulting system's response was preferable to that obtained from the higher order model. This is because uncertainties in the model parameters for higher orders have a destabilizing effect on the resulting controller obtained from pole-placement.

References

1 Astrom, K. J., Johnston, R. M:, and Sternby, J., 1984, "Zeros and Sampled Systems," *Automatica*, Vol. 20, pp. 31–38.

2 Craig, J. J., Hsu, P., and Sastry, S., 1986, "Adaptive Control of Mechanical Manipulators," IEEE Conference on Robotics and Automation, San Francisco, CA, Apr.

3 Goodwin, G. C., and Sin, K. S., 1984, *Adaptive Filtering Prediction and Control*, Prentice-Hall.

4 Jabbari, F., and Gibson, J. S., 1988, "Vector Channel Lattice Filters and Identification of Flexible Structures," *IEEE Transactions on Automatic Control*, May.

5 Landau, Y. D., 1979, *Adaptive Control*, Dekker.

6 Liu, S., and Bobrow, J., 1988, "An Analysis of a Pneumatic Servo System and Its Application to a Computer-Controlled Robot," ASME JOURNAL OF DYNAMIC SYSTEMS, MEASUREMENT, AND CONTROL, Sept.

7 Ljung, L., Soderstrom, T., 1983, *Theory and Practice of Recursive Identification*, The MIT Press.

8 Mannetje, J., 1981, "Pneumatic Servo Design Method Improves System Bandwidth Twenty-Fold," *Control Engineering*, June, pp. 79–83.

9 Nagarajan, V., 1988 "On-line Identification and Adaptive Control of a Pneumatic Robot Arm," MS thesis, Department of Electrical Engineering, University of California, Irvine.

10 Norton, P., 1985, *Programmer's Guide to the IBM PC*, Microsoft Press.

11 Ogata, K., 1970, *Modern Control Engineering*, Prentice Hall.

12 Rovner, D. R., 1987, "Experiments in Adaptive Control of a Very Flexible One Link Manipulator," PhD. dissertation, Stanford University, Aug.

13 Shearer, J. L., 1956, "Study of Pneumatic Process in the Continuous Control of Motion with Compressed Air–I," *Trans. of ASME*, Feb., pp. 233–242.

14 Slotine, J. E., and Li, W., 1987, "Adaptive Robot Control: A New Perspective," IEEE Conference on Decision and Control, Los Angeles, CA, Dec.

15 Sadegh, N., and Horowitz, R., 1987, "Stability Analysis of an Adaptive Controller for Robotic Applications," IEEE Conference on Robotics and Automation, Raleigh, NC Apr.